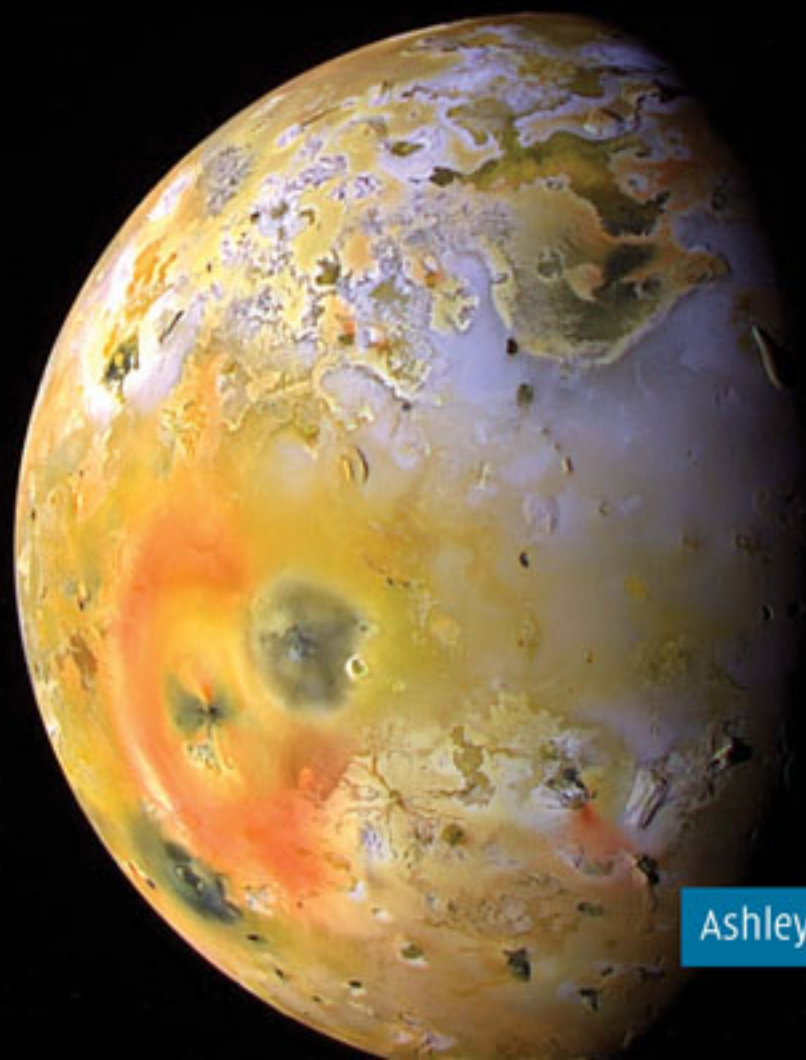


CAMBRIDGE PLANETARY SCIENCE

# Volcanism on Io

A Comparison with Earth



Ashley Davies



# VOLCANISM ON IO

## A Comparison with Earth

The most powerful volcanoes in the Solar System are found not on Earth but on Io, a tiny moon of Jupiter. Earth and Io are the only bodies in the Solar System with active, high-temperature volcanoes, but volcanoes on Io are larger and hotter – as well as more violent.

This book, the first dedicated to volcanism on Io, contains the latest results from the *Galileo* mission. In addition to investigating the different styles and scales of volcanic activity on Io, it compares those volcanoes to their contemporaries on Earth. The book also provides background on how volcanoes form and how they erupt, and explains quantitatively how remote-sensing data from spacecraft and telescopes are analyzed to reveal underlying volcanic processes.

This richly illustrated book will be a fascinating reference for advanced undergraduate and graduate students, as well as researchers in planetary sciences, volcanology, remote sensing, and geology.

ASHLEY DAVIES is a volcanologist at the Jet Propulsion Laboratory – California Institute of Technology in Pasadena, California. He was a member of the *Galileo* Near-Infrared Mapping Spectrometer Team, is Principal Investigator on several studies investigating volcanic activity on Io and Earth, and was a recipient of the 2005 NASA Software of the Year Award for his work on spacecraft autonomy.



# VOLCANISM ON IO

A Comparison with Earth

ASHLEY GERARD DAVIES

*Jet Propulsion Laboratory – California Institute of Technology*



CAMBRIDGE UNIVERSITY PRESS  
Cambridge, New York, Melbourne, Madrid, Cape Town, Singapore, São Paulo

Cambridge University Press  
The Edinburgh Building, Cambridge CB2 2RU, UK

Published in the United States of America by Cambridge University Press, New York

[www.cambridge.org](http://www.cambridge.org)

Information on this title: [www.cambridge.org/9780521850032](http://www.cambridge.org/9780521850032)

© A. G. Davies 2007

This publication is in copyright. Subject to statutory exception  
and to the provisions of relevant collective licensing agreements,  
no reproduction of any part may take place without  
the written permission of Cambridge University Press.

First published 2007

Printed in the United Kingdom at the University Press, Cambridge

*A catalogue record for this publication is available from the British Library*

*Library of Congress Cataloging in Publication data*

Davies, Ashley Gerard, 1961–

Volcanism on Io : a comparison with Earth / by Ashley Gerard Davies.

p. cm.

Includes bibliographical references and index.

ISBN-13: 978-0-521-85003-2

ISBN-10: 0-521-85003-7

1. Io (Satellite) – Volcanism. 2. Io (Satellite) – Volcanoes. 3. Planetary volcanism – Remote sensing.  
4. Volcanism. I. Title.

QB404.D38 2007

551.210999/25 – dc22 2006037426

ISBN-13 978-0-521-85003-2 hardback

# Contents

<i>Preface</i>	page xi
<i>List of Abbreviations</i>	xiii
<i>Reproduction Permissions</i>	xv
Introduction	1
<b>Section 1 Io, 1610 to 1995: Galileo to Galileo</b>	
1 Io, 1610–1979	7
1.1 Io before <i>Voyager</i>	7
1.2 Prediction of volcanic activity	9
1.3 <i>Voyager</i> to Jupiter	9
1.4 Discovery of active volcanism	12
1.5 IRIS and volcanic thermal emission	18
1.6 Io: the view after <i>Voyager</i>	19
1.7 Summary	24
2 Between <i>Voyager</i> and <i>Galileo</i> : 1979–1995	27
2.1 Silicate volcanism on Io?	27
2.2 Ground-based observations	29
2.3 Observations of Io from Earth orbit	33
2.4 The Pele plume	33
2.5 Outburst eruptions	34
2.6 Stealth plumes	37
2.7 Io on the eve of <i>Galileo</i>	38
3 <i>Galileo</i> at Io	39
3.1 Instrumentation	41
3.2 <i>Galileo</i> observations of Io	46
<b>Section 2 Planetary volcanism: evolution and composition</b>	
4 Io and Earth: formation, evolution, and interior structure	53
4.1 Global heat flow	53
4.2 Planetary formation	55

4.3	Post-formation heating	58
4.4	Interior structure	63
4.5	Volcanism over time	70
4.6	Implications	72
5	Magmas and volatiles	73
5.1	Basalt	73
5.2	Ultramafic magma	74
5.3	Lava rheology	76
5.4	Sulphur	78
5.5	Sulphur dioxide (SO <sub>2</sub> )	86
<b>Section 3 Observing and modeling volcanic activity</b>		
6	Observations: thermal remote sensing of volcanic activity	93
6.1	Remote sensing of volcanic activity on Earth	93
6.2	Remote sensing of volcanic activity on Io	95
6.3	Remote sensing of thermal emission	96
6.4	Blackbody thermal emission	97
6.5	Multi-spectral observations	98
6.6	The “dual-band” technique	99
6.7	Surface temperature distributions and effect on thermal emission	102
6.8	Hyperspectral observations	102
6.9	Analysis of hyperspectral thermal emission data	102
6.10	Analysis of SSI thermal emission data	107
7	Models of effusive eruption processes	108
7.1	Cooling of lava on Earth and Io	109
7.2	Modeling lava solidification and cooling	114
7.3	Volumetric rates ( $Q_F$ and $Q_E$ )	127
7.4	Models of lava emplacement	132
7.5	Supply to the surface: conduit geometry	134
7.6	Crustal structure controls on ascent of magma on Io	137
8	Thermal evolution of volcanic eruptions	142
8.1	Effusive activity: landforms and thermal emission evolution	143
8.2	Flux density as a function of eruption style	150
8.3	Summary	152
<b>Section 4 Galileo at Io: the volcanic bestiary</b>		
9	The view from <i>Galileo</i>	155
9.1	Surface changes: <i>Voyager</i> to <i>Galileo</i>	156
9.2	Color and composition	159

9.3	Discovery of widespread silicate volcanism	165
9.4	The rise (and fall?) of ultra-high-temperature volcanism	169
9.5	PPR observations	175
9.6	<i>Cassini</i> and <i>Galileo</i> observe Io	176
9.7	Adaptive optics and Hubble observations	176
9.8	Other discoveries	177
9.9	Summary	177
10	The lava lake at Pele	178
10.1	Setting	178
10.2	Observations of thermal emission	179
10.3	A lava lake at Pele	182
10.4	Importance of temporal and spectral coverage	183
10.5	Lava lakes	184
10.6	Implications for magma supply and interior structure	185
10.7	Plume composition and implications for volatile supply	185
10.8	Calculation of mass flux and flux densities	186
10.9	Further comparison with lava lakes on Earth	187
10.10	Summary	190
11	Pillan and Tvashtar Paterae: lava fountains and flows	192
11.1	Lava fountains: outbursts explained?	192
11.2	Pillan 1997: flood lavas and the emplacement of long flows	194
11.3	Tvashtar Paterae	200
11.4	Lava fountains on Io	201
11.5	Terrestrial analogues: flood basalts and fissure eruptions	202
11.6	Pillan comparisons with terrestrial eruptions	204
11.7	Summary: activity at Pillan in 1997 and at Tvashtar Paterae in 2000	205
12	Prometheus and Amirani: effusive activity and insulated flows	208
12.1	Volcanic activity at Prometheus	208
12.2	Comparison with Pu'u 'O'o-Kupaianaha, Hawai'i	213
12.3	Amirani flow field	215
12.4	Discussion and summary	216
13	Loki Patera: Io's powerhouse	217
13.1	<i>Voyager</i> to <i>Galileo</i>	218
13.2	Style of activity	219
13.3	Temporal behavior	220
13.4	Resurfacing of Loki Patera	222
13.5	Modeling the resurfacing process	225

13.6	Magma volume at Loki Patera	227
13.7	Summary: a class of its own	228
14	Other volcanoes and eruptions	229
14.1	Tupan Patera	229
14.2	Culann Patera and environs	230
14.3	Zamama	230
14.4	Gish Bar Patera	232
14.5	Emakong Patera: sulphur volcanism?	232
14.6	Balder and Ababinili Paterae: SO <sub>2</sub> flows?	234
14.7	The plumes of Surt and Thor	234
<b>Section 5 Volcanism on Io: the global view</b>		
15	Geomorphology: paterae, shields, flows, and mountains	239
15.1	Paterae on Io and calderas on Earth	239
15.2	Shield volcanoes	245
15.3	Lava flow morphology	249
15.4	Lava channels	250
15.5	Mountains and formation mechanisms	251
15.6	Conclusions	252
16	Volcanic plumes	253
16.1	Explosive activity on Io and Earth	253
16.2	Io observations	256
16.3	Plume types	257
16.4	Plume models	267
16.5	Summary	268
17	Hot spots	269
17.1	Variability and style of activity	270
17.2	Thermal emission comparisons	276
17.3	Effusion rates	277
17.4	Distribution of hot spots	278
17.5	Heat transport by eruption class	280
<b>Section 6 Io after <i>Galileo</i></b>		
18	Volcanism on Io: a post- <i>Galileo</i> view	287
18.1	Volcanism and crustal structure	287
18.2	Magma composition	288
18.3	Crust volatile content	289
18.4	Hot-spot variability	290
18.5	Eruption styles	290
18.6	Plumes	291
18.7	Volcanism on Io and Earth	292
18.8	Questions	292

19	The future of Io observations	294
19.1	Spacecraft observations	294
19.2	Imaging Io	298
19.3	Artificial intelligence, autonomy, and spacecraft operations	300
19.4	Telescope observations	302
	<i>Appendix 1 Io hot-spot locations</i>	305
	<i>Appendix 2 Io maps</i>	310
	<i>References</i>	317
	<i>Index</i>	341
	<i>Color plates follow page 210</i>	



# Preface

I have always been fascinated by volcanoes, and especially by Io, a tiny moon that beyond any expectation turned out to be the most volcanically active body in the Solar System. Now that the NASA *Galileo* mission is over and initial data analyses have been completed, this is an appropriate time to assess the “state of the satellite” and review what has been learned about Io over the past few decades.

A fascination with volcanoes is understandable, but I am also inspired to understand, through modeling of volcanic processes, how volcanoes *work*. Such motivation was instilled in me as a post-graduate student by Lionel Wilson and Harry Pinkerton at Lancaster University in the UK.

In this book, therefore, I have endeavored not only to describe what *Galileo* saw, but also to provide the necessary background for understanding the physical, volcanological processes taking place on Io, and to demonstrate how remote-sensing data of volcanic activity can be used to peel back the layers of a planet to reveal interior processes and structure. To put the majestic scale of volcanism on Io into proper context, comparison is made wherever possible with volcanic activity on Earth.

It has taken nearly two years to write this book. Along the way, I have had a great deal of help from friends, family, and colleagues. I thank Simon Mitton of Cambridge University Press, who originally suggested that I write this book and helped me prepare the proposal for Cambridge University Press; Diana Blaney, Nathan Bridges, Julie Castillo-Rogez, Torrence Johnson, Dennis Matson, Dave Pieri, and Glenn Veeder at the Jet Propulsion Laboratory, California Institute of Technology (JPL); Giovanni Leone and Lionel Wilson (Lancaster University); Laszlo Keszthelyi (U.S. Geological Survey [USGS] Astrogeology Branch), Jani Radebaugh (Brigham Young University), and Alison Canning Davies, all of whom reviewed chapters (multiple chapters in some cases); Tammy Becker (USGS) for supplying me with *Voyager* imagery; Paul Geissler (USGS) for a cylindrical projection of the magnificent Io global mosaic he helped create; Ju Zhang for

high-resolution images from his volcanic plume modeling; Bonnie Buratti (JPL), who gave me encouragement and sound advice over the years; my editors at Cambridge University Press, Jacqueline Garget and Susan Francis; and assistant editor Helen Morris. I wish also to thank Eleanor Umali of Aptara, Inc., and Dianne Scent for their invaluable help during the copyediting and indexing processes, and Mary Eleanor Johnson for her meticulous proofreading. My deepest thanks I reserve for my wife, Alison, who had to put up with me as I became more and more fixated on volcanoes and Io (well, more fixated than usual), and who was of immeasurable help, carefully reading, editing, and correcting text as it was written. This work I dedicate to her.

# Abbreviations

AIDA	Adaptive Image Deconvolution Algorithm
ALI	Advanced Land Imager ( <i>EO-1</i> )
AO	Adaptive optics
ASE	Autonomous Sciencecraft Experiment ( <i>EO-1</i> )
ASTER	Advanced Spaceborne Thermal Emission and Reflection Radiometer ( <i>Terra</i> )
CAI	Calcium-aluminum-rich inclusion
CRB	Columbia River Flood Basalts
CRISM	Compact Reconnaissance Imaging Spectrometers for Mars ( <i>MRO</i> )
ELT	Extremely Large Telescope
EOS	Earth Observing System
<i>EO-1</i>	<i>Earth Observing 1</i>
ESA	European Space Agency
ESO	European Southern Observatory
FLIR	Forward-looking infrared camera, built by FLIR Systems, Inc.
GEM	<i>Galileo</i> Europa Mission
GMM	<i>Galileo</i> Millennium Mission
<i>GOES</i>	<i>Geostationary Operational Environmental Satellite</i>
HGA	High Gain Antenna ( <i>Galileo</i> )
HiRise	High-Resolution Imaging Science Experiment ( <i>MRO</i> )
HRIR	High-Resolution Infrared Radiometer ( <i>Nimbus 1</i> )
HST	Hubble Space Telescope
IRIS	Infrared Radiometer Interferometer and Spectrometer ( <i>Voyager</i> )
IRTF	Infrared Telescope Facility
ISS	Imaging Sub-System ( <i>Cassini</i> )
ISS	Imaging Sub-System ( <i>Voyager</i> )
JPL	Jet Propulsion Laboratory, California Institute of Technology
LGA	Low Gain Antenna ( <i>Galileo</i> )

LLRI	Long-lived radioisotope
MODIS	Moderate-Resolution Imaging Spectroradiometer ( <i>Aqua</i> and <i>Terra</i> )
<i>MRO</i>	<i>Mars Reconnaissance Orbiter</i>
NASA	National Aeronautics and Space Administration
NGAO	Next Generation Adaptive Optics
NIMS	Near-Infrared Mapping Spectrometer ( <i>Galileo</i> )
OWL	Overwhelmingly Large telescope
PPR	Photo-Polarimeter Radiometer ( <i>Galileo</i> )
PPS	Photo-Polarimeter ( <i>Voyager</i> )
SLRI	Short-lived radioisotope
SSI	Solid State Imaging experiment ( <i>Galileo</i> )
SWIR	Short-wavelength infrared
TM	Thematic Mapper ( <i>Landsat</i> )
TMT	Thirty-Meter Telescope
UVS	Ultra-Violet Spectrometer ( <i>Voyager</i> )
UVS-EUVS	Ultra-Violet/Extreme Ultra-violet Spectrometer ( <i>Galileo</i> )
VLT	Very Large Telescope
WFPC2	Wide-Field Planetary Camera 2 (Hubble)

*Note: Spacecraft names are in italic.*

## Reproduction permissions

Figures 1.9a and 1.9b are from “Io” by Douglas B. Nash, Michael H. Carr, Jonathan Gradie, Donald M. Hunten, and Charles F. Yoder in *Satellites* by Joseph A. Burns and Mildred Shapley Matthews, editors. © 1986 The Arizona Board of Regents. Reprinted by permission of the University of Arizona Press.

Figure 5.4 is from “Dynamics and thermodynamics of volcanic eruptions: implications for the plumes on Io” by Susan Werner Kieffer in *Satellites of Jupiter* by David Morrison, editor. © 1982 The Arizona Board of Regents. Reprinted by permission of the University of Arizona Press.

The following material is reprinted with permission from Elsevier:

Plate 9e from *Icarus*, 169, Radebaugh, J. *et al.*, Observations and temperatures of Io’s Pele Patera from *Cassini* and *Galileo* spacecraft images, 65–79, © 2004;

Plate 7b from *Icarus*, 169, Lopes, R. *et al.*, Lava lakes on Io: Observations of Io’s volcanic activity from *Galileo* NIMS during the 2001 fly-bys, 140–174, © 2004;

Figures 3.2, 7.9, 7.10, and Plate 7a from *Icarus*, 148, Davies, A. G. *et al.*, Silicate Cooling Model Fits to *Galileo* NIMS Data of Volcanism on Io, 211–225, © 2000;

Figures 2.5, 7.5, 7.13, 7.14, and 8.5 from *Icarus*, 124, Davies, A. G., Io’s Volcanism: Thermo-Physical Models of Silicate Lava Compared with Observations of Thermal Emission, 45–61, © 1996;

Figures 7.15a, 7.15b, 7.16, and Plates 6d and 13a from *Icarus*, 184, Davies, A. G. *et al.*, The pulse of the volcano: the discovery of episodic volcanism at Prometheus on Io, 460–477, © 2006;

Figures 15.2a to 15.2c based on *Icarus*, 169, Keszthelyi, L. P. *et al.*, A post-*Galileo* view of Io’s interior, 271–286, © 2004;

Figure 15.4a from *Icarus*, 169, Schenk, P. *et al.*, Shield volcano topography and the rheology of lava flows on Io, 98–110, © 2004;

Figures 7.4, 7.6, 7.7, and Plates 10d and 11b from *Icarus*, 176, Davies, A. G., Post-solidification cooling and the age of Io's lava flows, 123–137, © 2005;  
Figure 9.4 from *Icarus*, 140, Geissler, P. *et al.*, Global color variations on Io, 265–282, © 1999;  
Figure 16.3 from *Icarus*, 169, Geissler, P. *et al.*, Surface changes on Io during the *Galileo* mission, 29–64, © 2004;  
Plate 14a from *Icarus*, 169, Turtle, E. *et al.*, The final *Galileo* SSI observations of Io: Orbits G28–I33, 3–28, © 2004;  
Plate 14b and 14c from *Icarus*, 163, Zhang, J. *et al.*, Simulation of gas dynamics and radiation in volcanic plumes on Io, 182–197, © 2003; and  
Figure 17.1 derived from *Icarus*, 176, Marchis, F. *et al.*, Keck AO survey of Io global volcanic activity, 96–122, © 2005.

Figure 6.7 is reproduced with permission from McEwen, A. *et al.*, High-temperature silicate volcanism on Jupiter's moon, Io, *Science*, 281, 87–90. © 1998 AAAS.

Figures 4.3 and 9.5 are reproduced with permission from *Jupiter*, Bagenal, F. *et al.*, editors. © 2004 Cambridge University Press.

# Introduction

*Volcanism: the manifestation at the surface of a planet or satellite of internal thermal processes through the emission at the surface of solid, liquid, or gaseous products.*

Peter Francis (1993), *Volcanoes: A Planetary Perspective*

Few geological phenomena inspire as much awe as a volcanic eruption. Eruptions are, quite frankly, extremely exciting to watch and experience. Could there then be any more exciting place to a volcanologist than the jovian moon Io ([Plate 1](#)), which has more active volcanoes per square kilometer than anywhere else in the Solar System? Io is the only body in the Solar System other than the Earth where current volcanic activity can be witnessed on such a wide scale. As a result of this high level of volcanic activity, Io has the most striking appearance of any planetary satellite.

The detection of an umbrella-shaped plume extending high above the surface of Io was the most spectacular discovery made by NASA's *Voyager* spacecraft during their encounters at Jupiter; in fact, it was one of the most important results from NASA's planetary exploration program. The discovery of active extraterrestrial volcanism meant that Earth was no longer the only planetary body where the surface was being reworked by volcanoes. With this exciting discovery a revolution in planetary sciences began, leaving behind the perception of planetary satellites as geologically dead worlds, where any dynamic process had been damped down into extinction over geologic time (billions of years).

The two *Voyager* spacecraft would continue through the Solar System on a grand tour of the gas-giant planets, passing Saturn, Uranus, and Neptune. More volcanic activity, this time cryovolcanic in nature, was discovered by *Voyager* on the neptunian moon Triton (Smith *et al.*, 1989; Kirk *et al.*, 1995). The *Cassini* spacecraft, which at the time of this writing was orbiting Saturn, has detected anomalies in the atmosphere of Titan that may indicate ongoing volcanic activity (Sotin *et al.*, 2005)

and active volcanism on Enceladus (Porco *et al.*, 2006). These planetary satellites are active, dynamic worlds. This realization began at Io.

This book is divided into six sections. [Section 1 \(Chapters 1 to 3\)](#) deals chronologically with Io observations and discoveries, which began at the very dawn of telescope-based astronomy in the seventeenth century; covers the discoveries made by technological masterpieces – the two *Voyager* spacecraft; and examines other studies of Io after *Voyager* and up to the arrival of the *Galileo* spacecraft at Jupiter at the end of 1995.

[Sections 2 and 3](#) provide essential background for understanding observations of volcanic activity. The dynamic nature of Io having been established, just why Io and Earth are so volcanically active today is examined in detail in [Section 2](#). [Chapter 4](#) summarizes current theories of formation and evolution of Earth and Io and the root causes of volcanism. [Chapter 5](#) then describes the genesis, properties, and behavior of magmas and the effects of dissolved volatiles, common on Io, on magma behavior.

[Section 3](#) covers how volcanoes on Io and Earth are studied using remote-sensing techniques and how mathematical models yield a quantitative understanding of volcanic activity. As noted by Peter Cattermole in his excellent book *Planetary Volcanism* (Cattermole, 1996), the exploration of volcanoes throughout the Solar System follows principles that are well known and fundamental to geology. For the specific case of understanding observations of volcanic activity from remote-sensing platforms, such investigations can be broken down into three stages.

The first stage consists of the acquisition of data, ideally at as high temporal, spatial, and spectral resolutions as possible. Visible-wavelength image data reveal volcanic plumes, lava flows, and surface morphology. Infrared data yield surface temperatures. Reflectance spectra are analyzed to reveal, or at least constrain, composition. Observations at shorter wavelengths, in the ultraviolet, detect molecular gas transitions. Accordingly, [Chapter 6](#) describes the remote-sensing techniques available for studying Io's volcanism.

The second stage of investigation involves the formation of a theory, based on all available data, of the physical processes involved that might explain the observations. From theory, a mathematical expression of the physical process is often developed. [Chapter 7](#) describes those models with a particular focus on understanding volcanism on Io.

The third stage of investigation consists of applying the models to data. To be an accurate representation of the process taking place, any model should be able to predict subsequent physical conditions. Once the accuracy of a model is established, it becomes a valuable tool for data interpretation. [Chapter 8](#) describes how different volcanic eruption styles can be identified from measurements of thermal emission.

Section 4 (Chapters 9 to 14) examines *Galileo*'s discoveries and looks at volcanic activity at individual locations: a tour of the volcano bestiary. *Galileo* revealed many different styles of volcanic activity taking place on Io, both effusive and explosive in nature. As on Earth, differences in magma composition, gas content, and tectonic setting play a role in the surface expression of volcanic activity. Where possible, Section 4 looks at individual volcanic centers, examines what was seen by *Galileo*, and then quantifies the volcanic processes using the techniques in Section 3. Volcanism on Io produces features that are familiar to terrestrial volcanologists: lava flows, lava lakes and ponds, pyroclastic deposits, and interactions between hot lava and surface volatiles. Where possible, ionian eruptions are quantitatively compared with similar styles of activity on Earth.

On Io, we observe volcanic activity on a scale that would be quite catastrophic on Earth, as well as processes that may have been extinct on Earth for millions and, in some cases, billions of years. By watching how eruptions in the extreme ionian environment evolve, we gain insight into similar terrestrial eruptions both today and in Earth's distant past. Resulting hypotheses and mathematical models, developed to explain extinct processes, can then be tested against new data of the process in action.

Every chapter in Section 4 highlights a different facet of Io's volcanism. Chapter 9 assesses the major discoveries made by *Galileo* and how the satellite had changed since *Voyager*. The next four chapters deal with very different expressions of volcanism at five locations:

- At Pele, an active, persistent lava lake;
- At Pillan and Tvashtar Paterae, rapidly emplaced lava fountains and voluminous flows;
- At Prometheus, an extensive insulated flow field emplaced over 16 years; and
- At Loki Patera, a quiescent, periodically overturning lava sea covering over 20 000 km<sup>2</sup>.

These are mostly familiar scenarios to a volcanologist, seen in many locations on Earth, but on Io they are on a vastly different scale. In the case of Loki Patera, there is no terrestrial analogue of this size, and there may never have been.

Different analyses performed at each location highlight a different technique of interpreting data of volcanic processes. In all cases, spectral signature constrains, to some extent, the lava emplacement or exposure mechanism. At Pele, the steadiness of wavelength of peak thermal emission is an important clue to the nature of activity. At Pillan, the modeling of variability in discharge rate yields clues to the emplacement of large, voluminous flows on Earth and Mars. At Prometheus, modeling the variability of effusion rate yields a picture of crustal structure and magma supply from a magma chamber. The temperature distribution at Loki Patera, derived from fitting data with thermal emission models, reveals the mechanism by which the patera is being resurfaced.

Chapter 14 looks at other ionian volcanoes and eruptions that exhibit other interesting facets of volcanic activity.

Section 5 summarizes, in a global context, Io's geomorphology (Chapter 15), volcanic plumes (Chapter 16), and hot spots (Chapter 17), including assessment of the role played by volcanism as a medium for transporting heat on Earth and Io.

Section 6 takes a broad look at Io after the *Galileo* mission, assesses what has been learned, and identifies the important questions raised after *Galileo* (Chapter 18). The prospects for future observations of Io that may answer these questions are covered in Chapter 19.

This book includes two appendices. Appendix 1 contains the locations of volcanic hot spots identified on Io. Appendix 2 contains maps of Io showing the locations of all named features.

# **Section 1**

Io, 1610 to 1995: Galileo to *Galileo*



# 1

## Io, 1610–1979

This chapter reviews the history of Io observations up to and including the *Voyager* encounters. The material in this chapter is drawn primarily from *Satellites of Jupiter* (Morrison, 1982) and *Satellites* (Burns and Matthews, 1986), both published by the University of Arizona Press, and *Time-Variable Phenomena in the Jovian System*, NASA Special Publication 494 (Belton *et al.*, 1989).

### 1.1 Io before *Voyager*

The study of Io dates from the very beginning of telescope-based astronomy. In his observation notes for January 7, 1610, Galileo Galilei wrote: “when I was viewing the heavenly bodies with a spyglass, Jupiter presented itself to me; and because I had prepared a very excellent instrument for myself I perceived that beside the planet there were three little stars, small indeed, but very bright.” Subsequent observations revealed a fourth “little star.”

Thus were discovered the Galilean satellites, named by Simon Marius (a contemporary of Galileo) Io, Europa, Ganymede, and Callisto. Subsequently, little attention was paid to the satellite system except as a means of measuring the speed of light (Roemer’s method). Not until the nineteenth century did physical observations become important. In 1805, Laplace used the orbital resonant properties to estimate satellite masses. New refracting telescopes at Lick and Yerkes measured satellite sizes, and bulk densities were obtained.

The development of photographic and photoelectric techniques in the early twentieth century led to the determination of satellite light curves, proved that all four Galilean satellites were in Jupiter-synchronous rotation (Stebbins, 1927; Stebbins and Jacobson, 1928), and led to the discovery of prograde and retrograde groups of smaller outer jovian satellites. Since the latter half of the twentieth century, larger telescopes and modern techniques of photometry, spectro-photometry, and polarimetry have been used to determine colors, albedoes, and more accurate values

of sizes and densities. Io was found to have the reddest surface in the Solar System (this work is summarized by Harris [1961]).

The occultation of a star by Io in 1971 yielded the first high-precision radius, 1818 km (Taylor *et al.*, 1971). Spectroscopy soon showed that water was a major component of the surface material of Ganymede and Europa (Pilcher *et al.*, 1972; Fink *et al.*, 1973) but was absent (down to the 1% level) on Io, already marked as being anomalous in the jovian system by its high albedo (0.6), red color, and post-eclipse brightening (first noticed by Binder and Cruikshank [1964]). In 1971, Sodium D line emission from Io was discovered (Brown, 1974) and a cloud of neutral sodium in the vicinity of Io was mapped (Trafton *et al.*, 1974; Trafton, 1975a), which led to the discovery of a potassium cloud (Trafton, 1975b). These features appeared to have their genesis on Io. The sputtering of material from the surface of Io by bombardment of charged particles trapped in the intense jovian magnetic field was proposed as the removal mechanism (Matson *et al.*, 1974).

The first spacecraft observations of the jovian system were made by *Pioneer 10* in 1973. The primary task of *Pioneer 10*, apart from proving the feasibility of deep-space missions, was the measurement of fields and particles in the spacecraft's environment. Particular attention was focused on the jovian magnetosphere, the most powerful planetary magnetosphere in the Solar System. Although few satellite measurements were made, improved values for satellite masses were calculated from analysis of *Pioneer's* trajectory through the jovian system (Anderson *et al.*, 1974). With a more accurate radius determination of 1815 km (Davies, 1982), the bulk density of Io was calculated to be  $3540 \text{ kg m}^{-3}$ , very similar to that of the Moon and indicating a composition dominated by silicates. A radio occultation of the spacecraft revealed that Io had an ionosphere or possibly an extended atmosphere (Kliore *et al.*, 1974, 1975). *Pioneer 10* also detected an extended hydrogen cloud near the orbit of Io (Judge and Carlson, 1974) as well as a high-energy flux tube linking Io to Jupiter. This flux tube was later found to be a control on Jupiter's decametric radio emission (Dessler and Hill, 1979; Desch, 1980). In December, 1974, *Pioneer 11* obtained a low-spatial-resolution image of Io from high above the north pole, showing that the northern hemisphere had some low-albedo areas.

In the wake of *Pioneer*, considerable attention was focused on the spectrum of Io. Wamsteker *et al.* (1974) were among those who noted a strong similarity between the spectrum of Io and that of sulphur, and it was proposed that sulphur was abundant on the surface of Io. Ionized sulphur emission from Io was discovered by Kupo *et al.* (1976). Spectral observations and laboratory work refined the Io spectrum and revealed a strong ultraviolet absorption feature, although the cause of this feature remained unknown until *Voyager* and laboratory work identified sulphur dioxide on the surface of Io.

Pre-*Voyager* spectral work is reviewed by Johnson and Pilcher (1977), and the reader is also directed to Cruikshank *et al.* (1977), Nash and Fanale (1977), Cruikshank *et al.* (1978), Pollack *et al.* (1978), and Fink *et al.* (1978).

The strong absorption feature in Io's spectrum at 4.1 microns ( $\mu\text{m}$ ), observed by Cruikshank *et al.* (1978) and Pollack *et al.* (1978), was identified from laboratory studies as sulphur dioxide in the form of a frost or adsorbate (Fanale *et al.*, 1979; Smythe *et al.*, 1979). Again, no water absorption bands were seen in telescope observations, demonstrating that Io's surface was water-ice-free and therefore very different from the water-rich surfaces of the other Galilean satellites.

### 1.2 Prediction of volcanic activity

Even prior to *Voyager*, it was evident from ground-based instruments that Io had unusual far-infrared photometry and radiometry, with higher brightness temperatures at 10  $\mu\text{m}$  than at 20  $\mu\text{m}$  (Morrison *et al.*, 1972) and unusual thermal inertia as Io emerged from eclipse (e.g., Hansen, 1973; Morrison and Cruikshank, 1973). These observations were difficult to interpret in the context of Io's being a dead, inactive world.

Just before the *Voyager 1* encounter with Io in March, 1979, a notable discovery was made. Witteborn *et al.* (1979) announced that an intense, temporary brightening at 2 to 5  $\mu\text{m}$  in the infrared had been observed, which they explained as an isolated surface area at a temperature of  $\approx 600$  K (on a planet where the peak daytime temperature is  $\approx 130$  K). Another hint of Io's dynamic nature came from Nelson and Hapke (1978), who suggested fumarolic activity as a possible mechanism for producing short-chain sulphur allotropes on Io's surface to explain features in Io's spectrum.

Only a few days before *Voyager 1* observed Io (and demonstrating exquisite timing), Peale *et al.* (1979) published an epochal paper on the heating of Io by tidal forces, in which they predicted "widespread and recurrent volcanism."

*Voyager* was to prove their theory spectacularly correct.

### 1.3 Voyager to Jupiter

Before the spinning *Pioneer 10* spacecraft had even reached Jupiter, development had already started on its successor. *Voyager* was based on the more sophisticated three-axis-stabilized *Mariner* spacecraft developed by NASA's Jet Propulsion Laboratory (JPL) in Pasadena, California. At launch, *Voyager* was eight times the weight of *Pioneer 10*, requiring NASA's most powerful available booster, the Titan IIIE, plus a Centaur upper stage to send it on its way to Jupiter. The *Voyager* project was developed as a multi-planet investigation of at least ten years' duration, for visiting

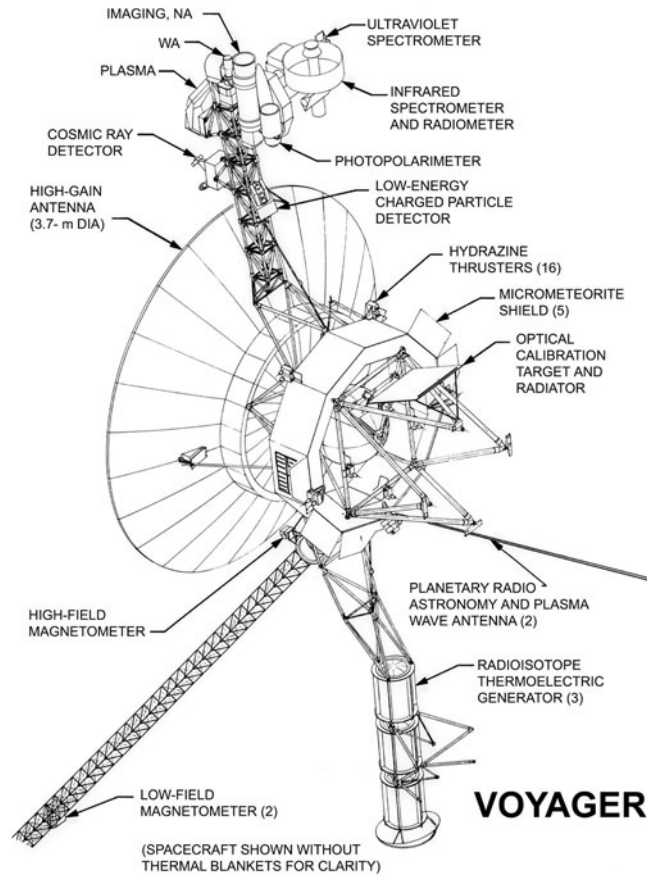


Figure 1.1 The fully deployed *Voyager* spacecraft. Courtesy of NASA.

Jupiter and Saturn and, hopefully, Uranus and Neptune as well: the long cherished “Grand Tour.”

Each *Voyager* spacecraft (Figure 1.1) weighed 815 kg in full deployment and carried three classes of instruments designed to collect information about the physical and chemical natures and radiation environments of 15 or more planetary bodies. The first group of instruments was mounted on a stabilized scan platform, a feature absent from the *Pioneer* design, which was essential to compensate for the speed of the spacecraft as it passed close to planets and their satellites. These instruments were two television cameras (imaging sub-system [ISS], not to be confused with the instrument with the same acronym on *Cassini*), one wide- and the other, narrow-angle; an infrared radiometer interferometer and spectrometer (IRIS); an ultra-violet spectrometer (UVS) to assess gas composition; and a photo-polarimeter (PPS) to measure molecular hydrogen, methane, and ammonia in planetary atmospheres.

Table 1.1 *Voyager Galilean satellite encounters*

Satellite	Closest approach (km)	Best resolution (km/line pair)
<i>Voyager 1</i>		
Io	20 570	1 <sup>a</sup>
Europa	733 800	33
Ganymede	114 700	2
Callisto	126 400	2
<i>Voyager 2</i>		
Io	1 129 900	20
Europa	205 700	4
Ganymede	62 100	1
Callisto	214 900	4

From Stone and Lane (1979a, 1979b).

<sup>a</sup> Best Io resolution limited by image smear.

Another set of instruments measured the strength of magnetic fields and the energies of charged particles: a plasma detector, a low-energy particle detector, two solid-state cosmic ray telescopes, and four magnetometers.

Finally, two 10-m antennas were used for radio astronomy experiments. The radio communications system was also used to sound planetary atmospheres and ionospheres by transmitting through them. All data were transmitted back to Earth at 23 W (watts) of power at rates up to 115.2 kB/s, to be received by stations of the Deep Space Network. Data were assembled, collated, and transmitted to JPL.

*Voyager 1* was launched on September 5, 1977, 16 days after *Voyager 2* (which was on a slower trajectory), and began substantive monitoring of the jovian system on January 6, 1979. Its closest approach to Jupiter was at a distance of 348 890 km on March 5, 1979. *Voyager 2* arrived at Jupiter 18 weeks later and encountered Jupiter at a perijove of 721 670 km on July 9, 1979 (Stone and Lane, 1979a, 1979b).

At Jupiter, the two *Voyagers* were on complementary trajectories. *Voyager 1* made close fly-bys of Io, Ganymede, and Callisto after perijove, making a south polar passage by Io (which would confirm the existence of the flux tube linking Io to Jupiter). *Voyager 2* made close approaches to Europa, Ganymede, and Callisto, but not Io (see Table 1.1), before perijove on a trajectory that would swing the spacecraft onto a course not only toward Saturn, but Uranus and Neptune as well.

*Voyager 1* passed by Io at a periapsis of 20 570 km (Table 1.1) and obtained images of moderate to high resolution (0.5–5 km/line pair) covering ≈40% of the surface (see Strom *et al.* [1981]). Table 1.2 shows the number of images taken as a function of resolution. The highest resolution images taken by *Voyager 1* were of the southern hemisphere of Io. *Voyager 2* took only low-spatial-resolution images of Io.

Table 1.2 *Total number of Voyager images of Io as function of image resolution*

Resolution/(km/line pair)	<0.5	0.5–2	2–5	5–20	>20
<i>Voyager 1</i>	33	96	75	61	278
<i>Voyager 2</i>	–	–	–	200	54

From Schaber (1982).

#### 1.4 Discovery of active volcanism

The images that *Voyager* returned of Io (Plate 2) revealed a world the likes of which had never been seen before. There were no impact craters, a ubiquitous feature of every other solid planetary and satellite surface in the Solar System that had been observed at resolutions where such features could be resolved. Io was multi-colored, with black, white, yellow, and red units. Broad plains were dotted with vents and calderas, and features of volcanic origin were identified, including long dark flows, broad dark flows, light flows (Smith *et al.*, 1979c), and reddish and white ring deposits. Isolated mountains reared up from the plains. This new, unexpected Io was full of surprises, the first of which was the discovery of active volcanism.

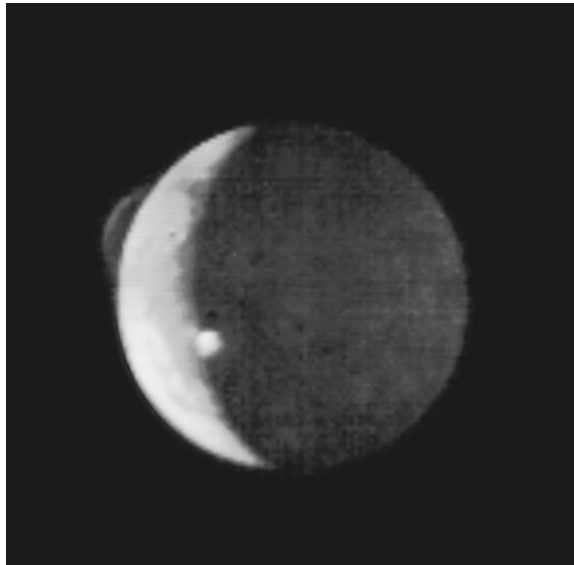


Figure 1.2 Discovery of volcanism on Io as seen by *Voyager 1* in an image obtained on March 8, 1979 (Morabito *et al.*, 1979). Two plumes are visible: the 260-km-high Pele plume on the limb and the plume at Loki illuminated on the terminator. (North is down.) Courtesy of NASA.

Table 1.3 Voyager 1 and Voyager 2 selected plume observations

Plume/site	Filter	Frame no.	Coordinates		Height <sup>a</sup> (km)	Width <sup>a</sup> (km)
			Long. W	Lat.		
1 Pele	C	16368.28 <sup>c</sup>	256.8°	19.4°S	298	1 214
1 Pele	UV	16368.50	256.8°	19.4°S	312	1 164
2 Loki	UV	20513.48 <sup>d</sup>	305.3°	19.0°N	382	–
2 Loki	C	20621.33	305.3°	19.0°N	148	445
3 Prometheus	C	16377.48	153.0°	2.9°S	77	272
4 Volund	V	16382.17	177.0°	21.5°N	98	–
4 Volund	UV	16382.23	177.0°	21.5°N	96	–
5 Amirani	C	16372.36	118.7°	27.2°N	114	184
5 Amirani	UV	16372.50	118.7°	27.2°N	137	387
6 Maui	C	16375.28	122.4°	18.9°N	68	343
6 Maui	C	20621.33	122.4°	18.9°N	76	185 <sup>b</sup>
7 Marduk	B	16389.21	209.7°	27.9°S	90	200 <sup>b</sup>
7 Marduk	UV	20608.01	209.7°	27.9°S	55	230 <sup>b</sup>
8 Masubi	C	20641.52	52.7°	45.2°S	64	177
9 Loki	C	16375.34	300.6°	16.9°N	16	–
9 Loki	C	20621.33	300.6°	16.9°N	35	–

From Strom *et al.* (1981).

Filters: C, clear; UV, ultra-violet; V, violet; B, blue, with wide-angle camera.

<sup>a</sup> Corrected for distance from limb.

<sup>b</sup> Uncorrected for limb position.

<sup>c</sup> Image numbers beginning with 1 taken by *Voyager 1*.

<sup>d</sup> Image numbers beginning with 2 taken by *Voyager 2*.

The first two volcanic eruption plumes were discovered by Morabito *et al.* (1979) in an image of Io (Figure 1.2) taken at 13:28 GMT on March 8, 1979, at a range of 4.5 million km. As part of the program to determine both the trajectory of the spacecraft and the ephemerides of the five innermost jovian satellites, the image was enhanced to determine the position of two faint stars. In doing so, a dim cloud of less than 10% of Io's brightness was revealed above the satellite's eastern limb, and another plume was seen catching the light on the terminator. When compared with the position of landforms observed on the satellite's surface, the former cloud was found to lie over, or nearly over, a 1400-km-diameter, heart-shaped feature centered at  $\approx 250^\circ$ W longitude and  $30^\circ$ S latitude that had already independently been identified as being of volcanic origin. This was the plume from the volcano Pele. In total, the two *Voyager* spacecraft discovered nine active plumes, which were named after deities and mythological characters associated with volcanoes, fire, and mayhem in general: Pele, Loki (two plumes, one of which is the terminator plume in Figure 1.2), Prometheus, Volund, Amirani, Maui, Marduk, and Masubi (see Table 1.3).

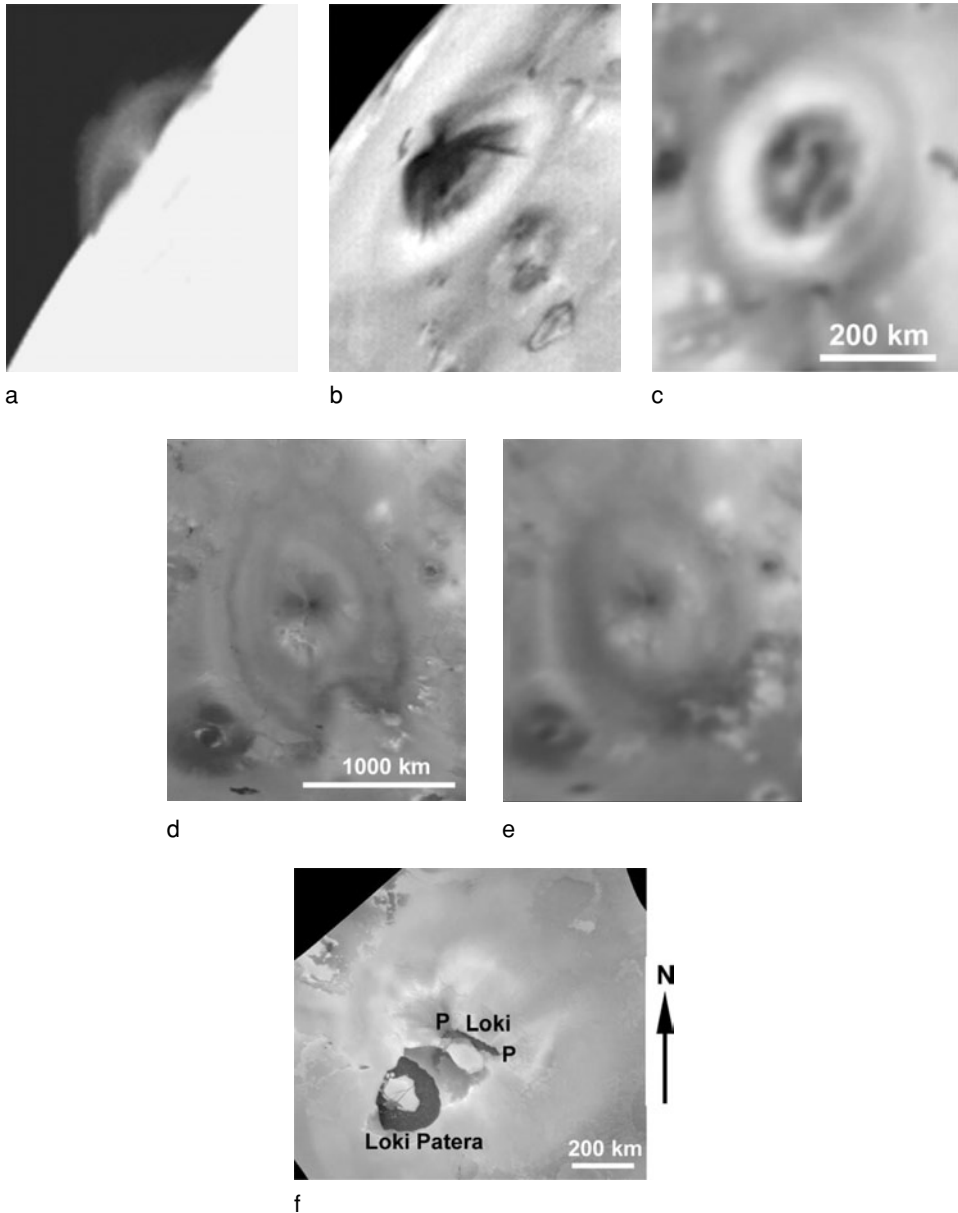


Figure 1.3 Plume and deposit classes as seen by *Voyager*: (a) and (b) The Prometheus plume is 75 km high, and structure in the plume implies the presence of some optically thick material. (c) The resulting bright annular surface deposits are approximately 300 km across. (d) The Pele plume laid down a deposit over 1200 km along the north–south axis and was active during the *Voyager 1* encounter. The unusual shape may have been caused by a vent obstruction impeding flow to the south. (e) By *Voyager 2*, the plume deposit had changed shape and the plume was not seen. It may be that the plume was mostly gas during this encounter, making direct observation difficult. (f) Loki, just north of the 200-km-diameter Loki Patera, was the site of two diffuse plumes (P), erupting from the ends of a possible fissure, that laid down irregular deposits. Courtesy of NASA.

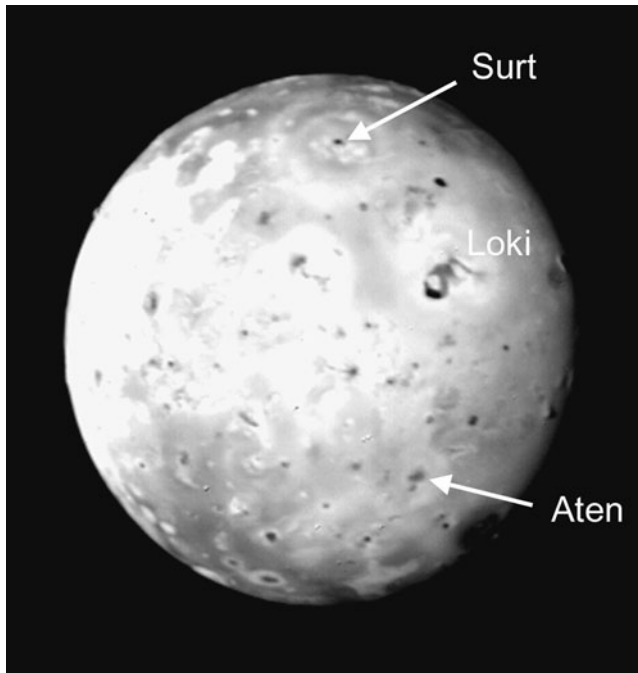


Figure 1.4 Between *Voyager 1* and *2* encounters, eruptions took place at Surt and Aten Paterae resulting in deposits similar to those at Pele. The absence of plumes at these sites led to the classification of Io's plumes into two main classes (McEwen and Soderblom, 1983). Pele-type plumes were larger, were from short-duration eruptions, were from hotter sources, and were dominated by sulphur, hence the darker deposits. Pele proved to have greater longevity than proposed by this model. Prometheus-type plumes were persistent, relatively small, and dominated by  $\text{SO}_2$ . Courtesy of NASA.

When *Voyager 2* arrived on the scene four months after *Voyager 1*, some obvious changes had taken place (Smith *et al.*, 1979b). The largest plume, Pele, had ceased erupting or activity had reached a level so meager as to remain undetected. Nevertheless, the pattern of Pele's ejecta blanket had been significantly altered (Figure 1.3). Six of the plumes *Voyager 1* had discovered were still erupting in very much the same way, and two (both in the vicinity of the Loki hot spot) had increased in size. There was also evidence to suggest that other eruptions on the scale of Pele had taken place at Surt and Aten Paterae (Figure 1.4) (McEwen and Soderblom, 1983), where giant Pele-like deposits had been laid down.

The volcanic plumes were best viewed against the background of space, where they showed up bright in contrast, but some were also seen against the planetary surface, where they appeared quite dark when compared with the average surface brightness. *Voyager 1* observed about 45% of the surface of Io in the limb regions, at a resolution of 10 km/line pair or better, and discovered eight plumes (Smith *et al.*, 1979c). In an attempt to place limits on the extent and duration of this type

Table 1.4 *Io hot spots identified from Voyager 1 IRIS data*

Feature	Long. (W)	Lat.	Area <sup>a</sup> (km <sup>2</sup> )	Temp <sup>a</sup> (K)	Total emitted				% of total hot-spot output
					Power emitted at 5 $\mu$ m (W)	Power emitted at 12 $\mu$ m (W)	Power emitted at 20 $\mu$ m (W)	Power emitted at 5 $\mu$ m (W) = % Io total <sup>b</sup>	
Loki Patera	309°	12°N	1 385	450	$2.77 \times 10^{11}$	$1.56 \times 10^{11}$	$7.73 \times 10^{10}$	$3.2 \times 10^{11}$	8.3
"			45 996	245	$4.37 \times 10^{10}$	$5.22 \times 10^{11}$	$1.82 \times 10^{12}$	9.4	24.1
Babbar Patera <sup>c</sup>	272°	40°S	88	322	$1.39 \times 10^9$	$3.27 \times 10^9$	$1.06 \times 10^7$	0.1	0.1
"			16 286	175	$1.41 \times 10^8$	$2.59 \times 10^{10}$	$4.53 \times 10^{11}$	0.9	2.2
Ulgen Patera <sup>c</sup>	289°	40°S	616	355	$2.23 \times 10^{10}$	$3.27 \times 10^{10}$	$1.87 \times 10^{10}$	0.6	1.4
"			19 113	191	$6.55 \times 10^8$	$5.41 \times 10^{10}$	$5.82 \times 10^{11}$	1.4	3.7
Svarog Patera <sup>c</sup>	268°	48°S	2 827	221	$7.49 \times 10^8$	$1.88 \times 10^{10}$	$8.92 \times 10^{10}$	0.4	1.0
Pele	256°	18°S	113	654	$1.68 \times 10^{11}$	$3.23 \times 10^{10}$	$1.32 \times 10^8$	1.2	3.0
"			20 106	175	$1.74 \times 10^8$	$3.20 \times 10^{10}$	$5.62 \times 10^{11}$	1.1	2.7
Amaterasu Patera	307°	38°N	5 000	283	$2.30 \times 10^{10}$	$1.10 \times 10^{11}$	$2.14 \times 10^{11}$	1.8	4.7
Amirani/Maui	120°	22°N	531	395	$4.36 \times 10^{10}$	$4.03 \times 10^{10}$	$1.61 \times 10^{10}$	0.7	1.9
"			7 543	200	$5.10 \times 10^8$	$2.83 \times 10^{10}$	$2.34 \times 10^{11}$	0.7	1.8
nr. NW Colchis	208°	31°N	254	385	$1.73 \times 10^{10}$	$1.78 \times 10^{10}$	$2.82 \times 10^9$	0.3	0.8
"			9 503	165	$3.03 \times 10^7$	$9.99 \times 10^9$	$2.45 \times 10^{11}$	0.4	1.0
Creidne Patera	344°	53°S	1 257	231	$5.85 \times 10^8$	$1.06 \times 10^{10}$	$3.50 \times 10^{10}$	0.2	0.5
nr. Nemea Planum	330°	81°S	908	225	$3.03 \times 10^8$	$6.65 \times 10^9$	$2.18 \times 10^{10}$	0.1	0.3
Mazda Paterae <sup>d</sup>	313°	9°S	60	420	$7.61 \times 10^9$	$5.51 \times 10^9$	$3.05 \times 10^5$	0.1	0.3
"			65 000	160	$1.20 \times 10^8$	$5.44 \times 10^{10}$	$1.68 \times 10^{12}$	1.4	3.5

Mbali Patera <sup>d</sup>	7°	31°S	2 000	159	0.04	$3.31 \times 10^6$	$1.60 \times 10^9$	$4.29 \times 10^{10}$	0.1
"			2	574	0.01	$1.60 \times 10^9$	$4.25 \times 10^8$	<1	0.03
Viracocha Patera <sup>d</sup>	281°	61°S	6 600	195	0.4	$3.08 \times 10^8$	$2.12 \times 10^{10}$	$1.98 \times 10^{11}$	1.1
Daedalus Patera <sup>d</sup>	275°	19°N	35 000	182	1.6	$5.70 \times 10^8$	$7.26 \times 10^{10}$	$1.02 \times 10^{12}$	4.1
Aten Patera <sup>d</sup>	310°	48°S	4 400	191	0.3	$1.51 \times 10^8$	$1.25 \times 10^{10}$	$1.26 \times 10^{11}$	0.7
Mihr/Gibil/Kibero Paterae <sup>d</sup>	294°–306°	15°–17°N	70 000	238	11.6	$4.70 \times 10^{10}$	$6.87 \times 10^{11}$	$2.69 \times 10^{12}$	29.7
Nusku Patera/ELT <sup>d,e</sup>	5°	65°S	2 500	170	0.1	$1.33 \times 10^7$	$3.25 \times 10^9$	$5.96 \times 10^{10}$	0.2
Creidne/Nusku Paterae <sup>d</sup>	5°–344°	53°–66°S	370	354	0.3	$1.31 \times 10^{10}$	$1.95 \times 10^{10}$	$6.91 \times 10^9$	0.8
"			11 000	155	0.2	$1.14 \times 10^7$	$7.23 \times 10^9$	$2.68 \times 10^{11}$	0.5
Unnamed active center <sup>d</sup>	≈334°	≈12°N	7 000	186	0.4	$1.60 \times 10^8$	$1.67 \times 10^{10}$	$2.01 \times 10^{22}$	0.9
ELT <sup>d</sup>	280°	75°S	2 800	175	0.1	$2.42 \times 10^7$	$4.46 \times 10^9$	$6.99 \times 10^{10}$	0.3
ELT <sup>d</sup>	50°	75°S	10	417	0.02	$1.21 \times 10^9$	$8.99 \times 10^8$	<1	0.0
"			86 000	63	0.1	<1	$7.02 \times 10^5$	$8.77 \times 10^{11}$	0.2
<b>Total</b>					<b>39.0</b>				<b>100</b>

<sup>a</sup> Temperatures and areas from Pearl and Sinton (1982), except for Amaterasu (Pearl, 1985) and hot spots discovered by McEwen *et al.* (1996); see note *d*.

<sup>b</sup> Total Io thermal output= $10^{14}$  W (Veeder *et al.*, 1994).

<sup>c</sup> Ulgen, Babbar, and Svarog were combined into one hot spot due to IRIS footprint location and size by McEwen *et al.* (1989). The shading of the % of total hot-spot output column denotes this combination.

<sup>d</sup> Hot spots identified in IRIS data by McEwen *et al.* (1992; 1996). Power output per unit area determined using  $\sigma(T^4 - 130^4)$  for areas where  $T > 130$  K.

<sup>e</sup> ELT=eroded layered terrain (also called eroded layered plain).

of volcanic activity, the *Voyager 2* imaging system observed Io intermittently over a five-day period, including a continuous eight-hour “volcano watch.” *Voyager 2* observed 80% of the surface on the limb, which with the *Voyager 1* observations brought the total coverage to nearly 100%. All plumes greater than 100 km in height that were active during the encounters were probably recorded in this way; most were seen several times (Smith *et al.*, 1979c). No plume activity was observed at high latitudes, nor were any polar ice caps found. Indeed, the poles of Io were dark and reddish (Dollfus, 1975; Murray, 1975; Graham and Hapke, 1986).

### 1.5 IRIS and volcanic thermal emission

The *Voyager* IRIS observed approximately 30% of the surface of Io at resolutions between 70 km and 700 km, with the best resolution at high southern latitudes (Pearl and Sinton, 1982). *Voyager 2* was too far from Io to take any usable IRIS readings.

IRIS obtained useful spectra from wavelengths of 4  $\mu\text{m}$  to 55  $\mu\text{m}$  (Hanel *et al.*, 1979). The fields of view appeared on the Io surface as circular footprints ranging from 250 km to 1000 km in diameter. Uncertainties in the pointing of the *Voyager* scan platform resulted in possible errors in footprint locations on the surface of about half a footprint diameter when concurrent imaging was available, and larger possible errors otherwise (McEwen *et al.*, 1985). Probably the most valuable contribution IRIS made during the Jupiter system encounter was the identification of individual hot spots associated with areas of intense volcanism on Io (Smith *et al.*, 1979c). Major hot spots identified in IRIS data are shown in Table 1.4.

Co-registering IRIS and imaging data showed that some of these hot spots were relatively dark-floored calderas (albedo  $<0.3$ ) with temperatures less than 400 K, although a small area  $>600$  K at the base of the Pele plume was identified. Detailed modeling of these data showed that Pele IRIS data could be best fitted with a three-component fit. The highest temperature was at least 654 K, with a very small area (Figure 1.5) (Pearl and Sinton, 1982). This was the highest temperature derived from IRIS data and hinted at the possible presence of silicate volcanism.

IRIS also detected sulphur dioxide in the Loki plume (Pearl *et al.*, 1979a), determining the driving volatile for at least some of the plumes.

Hot spots and plumes were soon assigned names and associated, where possible, with a surface feature. The low spatial resolution of IRIS meant that in some cases determining the location of the thermal emission was difficult, with multiple sources in the IRIS field of view. Loki was a case in point. The Loki plumes issued from the ends of what appeared to be a fissure, and this was logically the source of the thermal emission; however, just to the south of the fissure and within the IRIS field of view was Loki Patera, which had the appearance of a huge, 200-km-diameter lava lake and another likely source of the thermal emission detected by IRIS.

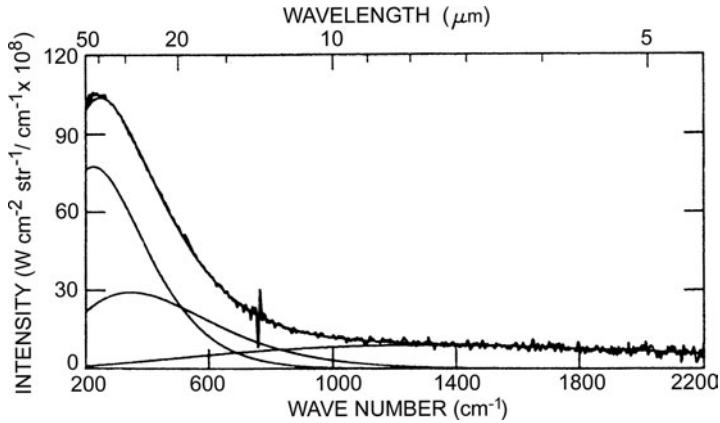


Figure 1.5 *Voyager 1* IRIS spectrum of the Pele region. The smooth curve fitted to the data is the sum of three temperatures and fractions of the IRIS field of view at 114 K (0.899), 175 K (0.100), and 654 K ( $5.77 \times 10^{-4}$ ) by Pearl and Sinton (1982). IRIS was not sensitive to smaller areas at hotter temperatures. A temperature of 654 K is too hot for liquid sulphur to be stable on the surface. The feature at 12  $\mu\text{m}$  is an artifact.

## 1.6 Io: the view after *Voyager*

### 1.6.1 Surface features

The *Voyager* spacecraft revealed an Io that was unlike any other planetary surface known at the time, with a morphology and composition dominated by volcanism. This was a decade before the *Magellan* mission would reveal the volcanism-dominated surface of Venus. Not a single impact crater was seen even in the highest resolution images (in which a crater 1 km to 2 km in diameter could have been identified). Instead, over 100 caldera-like depressions up to 200 km in diameter were identified (Smith *et al.*, 1979a). These features were named “paterae” (see Figures 1.6 and 1.7). Some paterae and escarpments were 1–3 km deep (Arthur, 1981; Schaber, 1982; Davies and Wilson, 1987) and some had complex radiating flows. Smith *et al.* (1979c) concluded that Io was being resurfaced by volcanic processes at a prodigious burial rate, later estimated to be  $0.1 \text{ cm year}^{-1}$  to  $10 \text{ cm year}^{-1}$  (Johnson *et al.*, 1979; Johnson and Soderblom, 1982). This explained the absence of impact craters, which are being rapidly buried.

A geologic map covering about a third of Io’s surface was created from high- and moderate-resolution *Voyager 1* images (Masursky *et al.*, 1979; Schaber, 1980, 1982). The wide array of landforms and albedo features was divided into three main broad categories: mountains, plains, and vent regions (Carr *et al.*, 1979; Smith *et al.*, 1979c; Schaber, 1982).

*Voyager* saw mountains as high as 9 km and more than 200 km across, such as Haemus Montes (Figure 1.7). Such high relief pointed to a composition

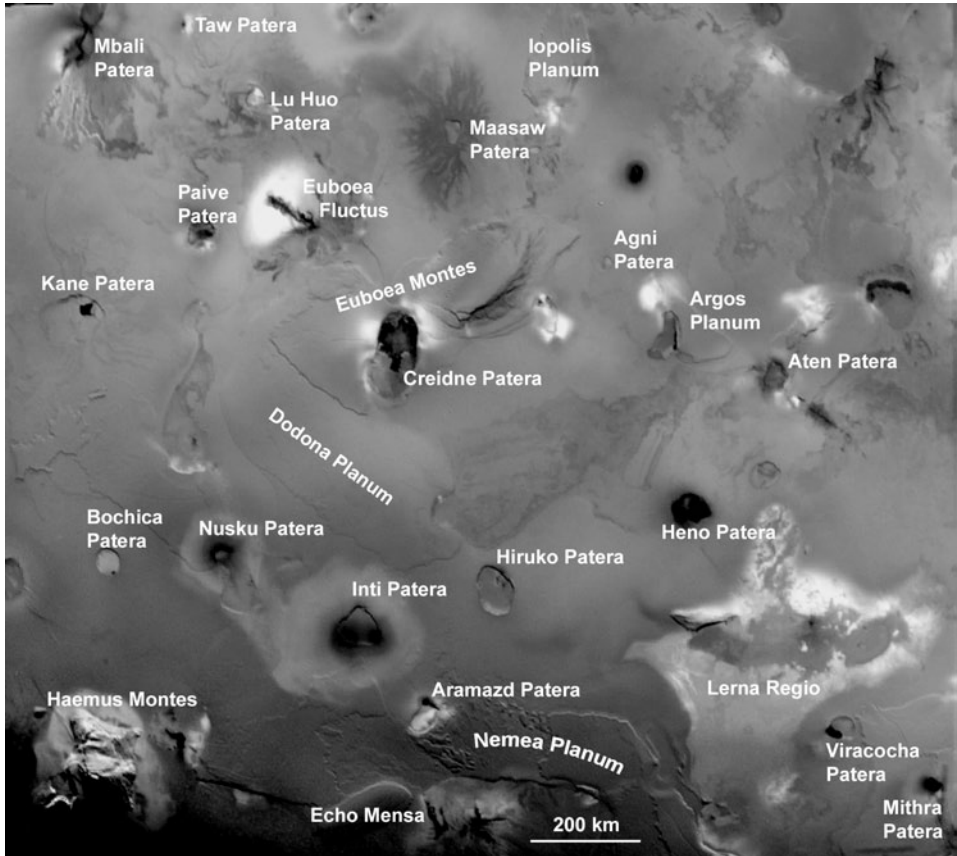


Figure 1.6 One of the best images of Io obtained by *Voyager 1* of the south polar region from longitude 270°W to 60°W and latitude 30°S to 85°S. The image contains a plethora of surface features and different morphologies including shield-like volcanoes with nested craters and radiating flows; other deep, steep-walled paterae set into flat plains; eroded plains; and jagged mountains, indicative of a predominantly silicate lithosphere. *Voyager* Wide Angle camera image FDS 16392.39. Courtesy of NASA.

predominantly of silicate material (Clow and Carr, 1980). The surface of the mountains appeared to be tectonically disrupted, with the mountain blocks exhibiting massive fracturing. The mountains north of Creidne Patera had lobate scarps that resembled large landslides, which may have been fault-controlled. Some mountains were possibly volcanic in origin, surrounded in some cases by bright aureoles (Haemus and Boösaule Montes, for example). Others were interpreted in the 1980s as exposures of silicate lithosphere that elsewhere were covered by sulphur deposits (Carr, 1986).

Plains were divided into three classes: inter-vent plains, layered plains, and eroded layered plains (also called eroded layered terrains). Multi-colored units (in exaggerated color images) ranged in hue from yellow and orange to red-brown.

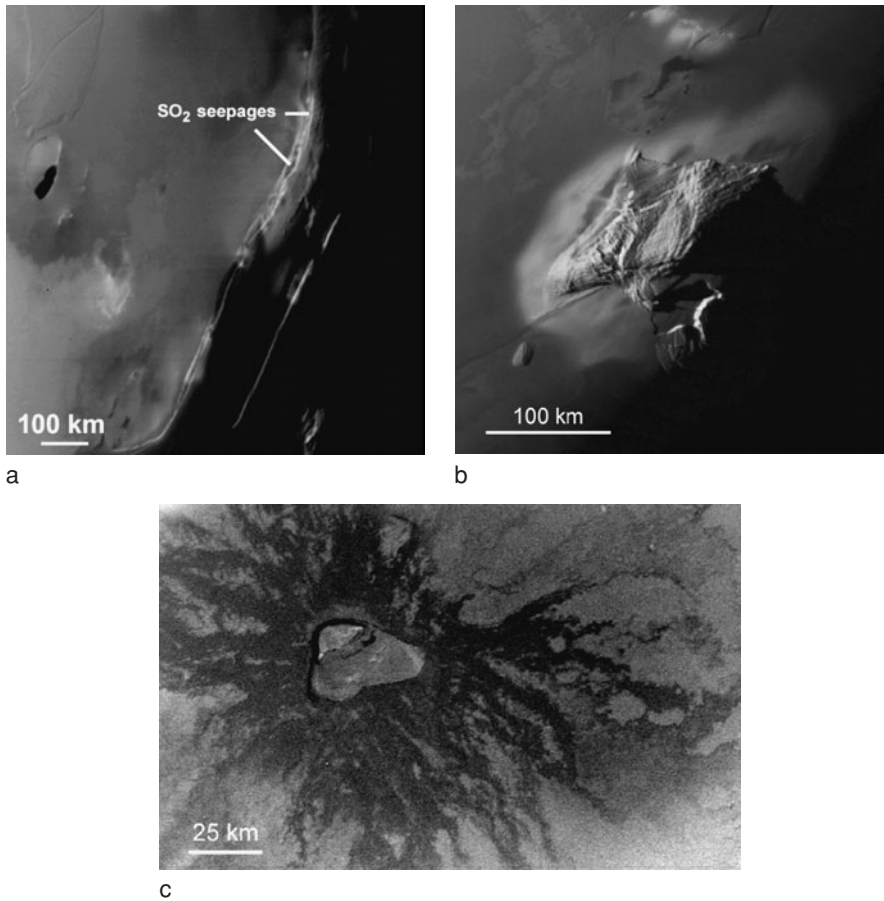


Figure 1.7 Details of selected features on the surface of Io as imaged by *Voyager 1*: (a) south polar region scarps in layered plains with seepages of  $\text{SO}_2$ ; (b) Haemus Montes, a block of mountains  $\approx 9$  km high; (c) Maasaw Patera,  $\approx 25$  km  $\times$  35 km in size and  $\approx 2$  km deep, has a nested caldera similar to some terrestrial and martian volcanoes. Courtesy of NASA.

Inter-vent plains made up  $\approx 40\%$  of the mapped area and had relatively smooth surfaces, with an albedo that was regionally consistent. In the highest-resolution images, the plains were seen to contain abundant low relief scarps, both straight and sinuous (Figure 1.7). The inter-vent plains unit was thought to be composed of stratified materials of volcanic plume fallout, smaller-scale fumarole deposits, and material emplaced effusively from volcanic vents.

Layered plains appeared as extensive, flat plains with boundary scarps ranging in height from 500 m to 1700 m. This terrain was most markedly developed near the south pole. Layered plain boundaries were thought to be temporary erosion boundaries with the main erosion agent being sulphur dioxide (McCauley